Remote Sensing and Hydrology 2000 (Proceedings of a symposium held at Santa Fe, New Mexico, USA, April 2000). IAHS Publ. no. 267, 2001.

Estimation of surface emissivity for arid lands

THOMAS SCHMUGGE, ANDREW FRENCH, JERRY RITCHIE & ALBERT RANGO

USDA ARS Hydrology Laboratory, BARC-W, Beltsville, Maryland 20705, USA

e-mail: schmugge@hydrolab.arsusda.gov

Abstract Knowledge of surface emissivity is important for determining the radiation balance at the land surface. For heavily vegetated surfaces there is little problem since the emissivity is relatively uniform and close to one. For arid lands with sparse vegetation the problem is more difficult because the emissivity of the exposed soils and rocks is highly variable. With multispectral thermal infrared (TIR) observations it is possible to estimate the spectral emissivity variation for these surfaces. The data presented is from the TIMS (Thermal Infrared Multispectral Scanner) instrument which has six channels in the 8 to 12 μm region. TIMS is a prototype of the TIR portion of the ASTER (Advanced Spaceborne Thermal Emission and Reflection radiometer) instrument on NASA's EOS-TERRA satellite. The approach is to use the Temperature Emissivity Separation (TES) algorithm developed for use with ASTER data to extract the temperature and six emissivities from the six channels of TIMS data. The algorithm makes use of the empirical relation between the range of observed emissivities and their minimum value. This approach was applied to the TIMS data acquired over the USDA/ARS Jornada Experimental Range in New Mexico. The Jornada site is typical of a desert grassland where the main vegetation components are grass (black grama) and shrubs (primarily mesquite) in the degraded grassland. The data are from an altitude of 800 m yielding a pixel resolution of approximately 2 m. The resulting spectral emissivities are in qualitative agreement with laboratory measurements of the emissivity (ε) for the quartz rich soils of the site with $\varepsilon < 0.8$ for the 8–9.5 μm channels. For the longest wavelength channel little spatial variation of ε was observed with values of 0.96 ± 0.005 over large areas.

Key words arid lands; ASTER; Chihuahuan Desert; emissivity; Jornada; multispectral; surface temperature; thermal infrared; TIMS

INTRODUCTION

The thermally emitted radiance from any surface depends on two factors: (a) the surface temperature, which is an indication of the equilibrium thermodynamic state resulting from the energy balance of the fluxes between the atmosphere, surface and the subsurface soil; and (b) the surface emissivity which is the efficiency of the surface for transmitting the radiant energy generated in the soil into the atmosphere. The latter depends on the composition, surface roughness, and physical parameters of the surface, e.g. moisture content. In addition, the emissivity generally will vary with wavelength for natural surfaces. Thus to make a quantitative estimate of the surface temperature we need to separate the effects of temperature and emissivity in the observed radiation. An approach for doing this with multispectral thermal infrared data is presented and demonstrated with data acquired over the Jornada Experimental Range in New Mexico (USA).

THERMAL RADIATION

The intensity of the thermal radiation from an object is described by the Planck black body relationship given as a function of wavelength in equation (1):

$$L_{BB}(\lambda,T) = \frac{2hc^2/\lambda^5}{\exp(hc/\lambda kT)-1} \quad (1)$$

where h is Planck's constant (6.626×10^{-34} J s^{-1}), c is the speed of light (2.998×10^{8} m s^{-1}) and k is Boltzmann's constant (1.381×10^{-23} J K^{-1}). The units are W m^{-2} sr^{-1} m^{-1}. At common terrestrial temperatures (300 K) the peak emission occurs in the 8 to 10 μm range of wavelength. It is fortuitous that this peak occurs in a wavelength region where the atmosphere is relatively transparent compared to adjacent wavelengths. While the peak in atmospheric transmission is in the 8 to 12 μm range, there is still significant attenuation due primarily to water vapour. As a result the magnitude of the atmospheric effect will depend on the water vapour content of the intervening atmosphere. This unknown or uncertain atmospheric contribution is one of the problems for the remote sensing of surface temperature at infrared wavelengths.

The data presented here were obtained with the Thermal Infrared Multispectral Scanner (TIMS) sensor on board a DOE Cessna Citation aircraft on 30 September 1997. TIMS has six channels in the thermal infrared (8–12 μm) region of the electromagnetic spectrum. The six channels are portrayed graphically in Fig. 1 along with laboratory measurements of the emissivity for three soils from the Jornada. It is clear that there will be a variation of the emissivity over the six TIMS channels for these soils. The instantaneous field of view is 2.5 mrad. Thus from the altitude of 800 m the pixel size is 2 m.

The radiances measured at the aircraft are given by:

$$L_j(surf) = (L_j(a/c) - L_j(atm\uparrow)) / \tau_j \quad (2)$$

where the values of the atmospheric transmission, τ_j, and upwelling radiation, $L_j(atm\uparrow)$, can be calculated using atmospheric radiative transfer, e.g. MODTRAN, with atmospheric profile data measured at the nearby White Sands missile range. The remaining problem is to relate these radiances to the surface emissivity in the six channels without direct knowledge of the temperature, T_{grd}, using the relation:

$$L_j(surf) = \varepsilon_j\, BB_j(T_{grd}) + (1-\varepsilon_j)\cdot L_j(atm\downarrow) \quad (3)$$

where $BB(T)$ is the Planck equation for the radiation from a black body as given by equation (1).

TEMPERATURE/EMISSIVITY RECOVERY

Equation (3) indicates that if the radiance is measured in n spectral channels, there will be n+1 unknowns: the n emissivities and the surface temperature. The set of equations described by the radiance measurements in n spectral channels is thus under determined, and additional information is needed in order to extract either the temperature or the emissivity information. This has led to the development of a variety of techniques which differ according to the assumptions that they make. The technique

used here is that which is being used with data from the Advanced Spaceborne Thermal Emission Reflectance Radiometer (ASTER) on the Earth Observing System Platform, TERRA launched in December 1999 (Yamaguchi *et al.*, 1998). This approach makes use of an empirical relation between the range of emissivities and the minimum value for a set of multichannel observations. It is termed Temperature Emissivity Separation or TES (Gillespie *et al.*, 1998). The estimated kinetic temperature, T, is taken to be the maximum T estimated from the radiances for the n spectral channels calculated from equation (3) using an assumed emissivity value (ε) typically 0.97, so that surface types (vegetation, snow, water, soil and rock), will all be within ±0.03 of the chosen value. Relative emissivities, β_j are found by ratioing the acquired radiance data, corrected for atmospheric effects to the average of all channels:

$$\beta_j = \frac{L_j}{\overline{L}} \frac{\overline{BB}}{BB(T)_j} = \frac{\varepsilon_j}{\overline{\varepsilon}} \tag{4}$$

In principle β_j may range widely. However, since the emissivities are generally restricted to 0.7–1.0, the ratioed values are restricted to 0.7–1.4. The β_j values provide a temperature independent index which can be matched against β_j values calculated from laboratory/field measurements of natural materials. In the TES method the max-min difference ($MMD = \max(\beta_j) - \min(\beta_j)$) is related to the minimum emissivity. From laboratory measurements of emissivities (Salisbury & D'Aria, 1992) the relationship between ε_{min} and MMD was found to be:

$$\varepsilon_{\min} = 0.994 - 0.687 \times MMD^{0.737} \tag{5}$$

and can be used to calculate the emissivities from the β spectrum:

$$\varepsilon_j = \beta_j \left(\frac{\varepsilon_{\min}}{\min(\beta_j)} \right) \tag{6}$$

The β_j are determined from the measured surface radiances L_j. From these ε_j a new temperature can be obtained and the process repeated until the results converge, which usually occurs after two or three iterations. A limitation of the method is that the smallest value of MMD is determined by instrument noise and the quality of atmospheric correction. This will affect the maximum ε that will be observed in the scene.

THE JORNADA SITE

The Jornada Experimental Range lies between the Rio Grande flood plain (elevation 1190 m) on the west, and the crest of the San Andres mountains (2830 m) on the east. The Jornada is 783 km^2 in area and is located 37 km north of Las Cruces, New Mexico on the Jornada del Muerto Plain in the northern part of the Chihuahuan Desert. The larger Jornada del Muerto basin is typical of the Basin and Range physiographic province of the American southwest and the Chihuahuan Desert.

Three specific sites in the Jornada were chosen for intensive studies. Sites were selected to represent grass, shrub (mesquite), and grass-shrub transition areas. The grass site is in a fairly level area where black grama dominates and encompasses an exclosure where grazing has been excluded since 1969. Honey mesquite on coppice

dunes dominates the shrub site. The dunes vary in height from 1 to 4 m with honey mesquite on each dune. Bare soil dominates the lower areas between these coppice dunes. The transition site has vegetation components from both the grass and shrub sites. We will present results from the grass and shrub sites in this paper. Soil samples from several of the sites were taken to the Jet Propulsion Laboratory for measurements of their emissivity spectra. The results for soils from the mesquite and grass sites are shown in Fig. 1 along with the TIMS spectral response functions. The integrated values of the emissivity for each channel are given in Table 1. We note that shortest wavelength channels, 1, 2 and 3, have the largest variation (>0.2) for the four samples. While the longest wavelength channel, 6, has an order of magnitude less variation (0.008).

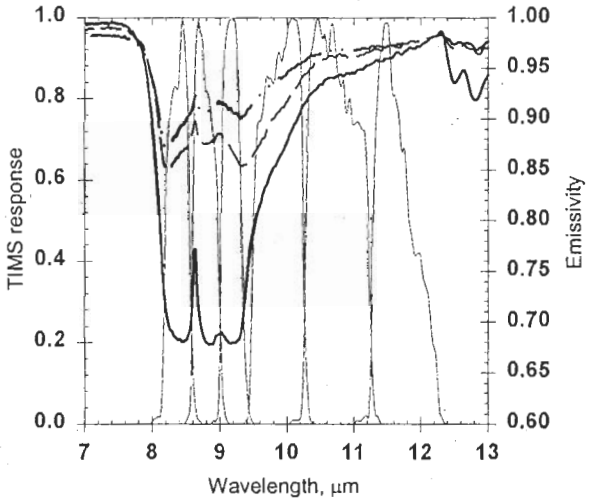

Fig. 1 Plots of the TIMS spectral response functions and laboratory measurements of the emissivity for three soils from the Jornada. The TIMS channels are numbered 1–6 from the left. The upper emissivity curve is for soil from the grass site, the middle is for dark red soil from the mesquite site and the bottom curve is for light sandy soil from the same site.

Table 1 Jornada soils' emissivities for the six TIMS channels.

Soil/Site	Chan 1 8.47 μm	Chan 2 8.94 μm	Chan 3 9.34 μm	Chan 4 9.96 μm	Chan 5 10.80 μm	Chan 6 11.74 μm
Transition	0.820	0.830	0.826	0.907	0.955	0.971
Light sand/Mesquite	0.697	0.687	0.700	0.873	0.942	0.967
Dark sand/Mesquite	0.871	0.879	0.863	0.914	0.961	0.973
Crust/Grass	0.897	0.911	0.907	0.943	0.968	0.975

RESULTS

Figure 2 presents a sample of the results from the 30 September 1997 flight. Images of the channel 1 emissivity are presented for the grass and mesquite sites. For the grass site the emissivity is relatively uniform except for the exposed soils along the roads and a couple of bare patches. The exclosure mentioned above is apparent to the left of

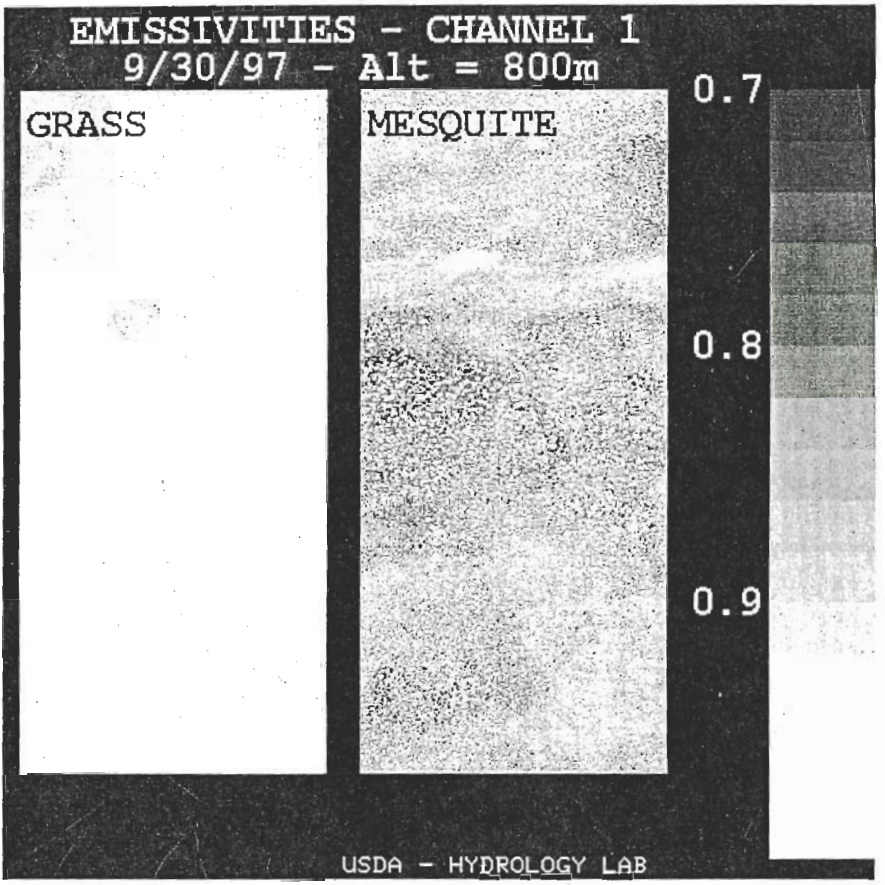

Fig. 2 Images of the channel 1 emissivity for both the grass and mesquite sites using data acquired on 30 September 1997. North is up on these images which are 2.7 km long and 0.9 km across.

the road in the middle of the image. The area inside the exclosure shows the most uniform and highest emissivities. The results for the mesquite site show almost the opposite results, i.e. mostly low emissivities due to the exposed soil between the mesquite dunes. The white spots are the mesquite bushes which have high emissivities. These results are quantified in Fig. 3 which presents histograms for each of the six channels at the two sites. For the grass site the histogram is for an area within the exclosure, while for the mesquite it is for a much larger area covering the complete swath in the middle of the image. For the mesquite site the short wavelength channels, 1–3, show a double peaked distribution indicative of pure soil pixels ($\varepsilon \sim 0.8$) in reasonable agreement for a mixture of the light and dark sands from the laboratory measurements, and a second smaller but sharper peak at $\varepsilon \sim 0.98$ indicative of pure vegetation pixels. In fact all six channels show this peak. For channel 6 all the pixels are between 0.96 and 0.98, with a sharp cut-off at the lower end as expected because of the high emissivity for the soils at this wavelength. For the grass site all six distributions are much tighter, with none of them showing the low emissivity behaviour expected for pure soil pixels.

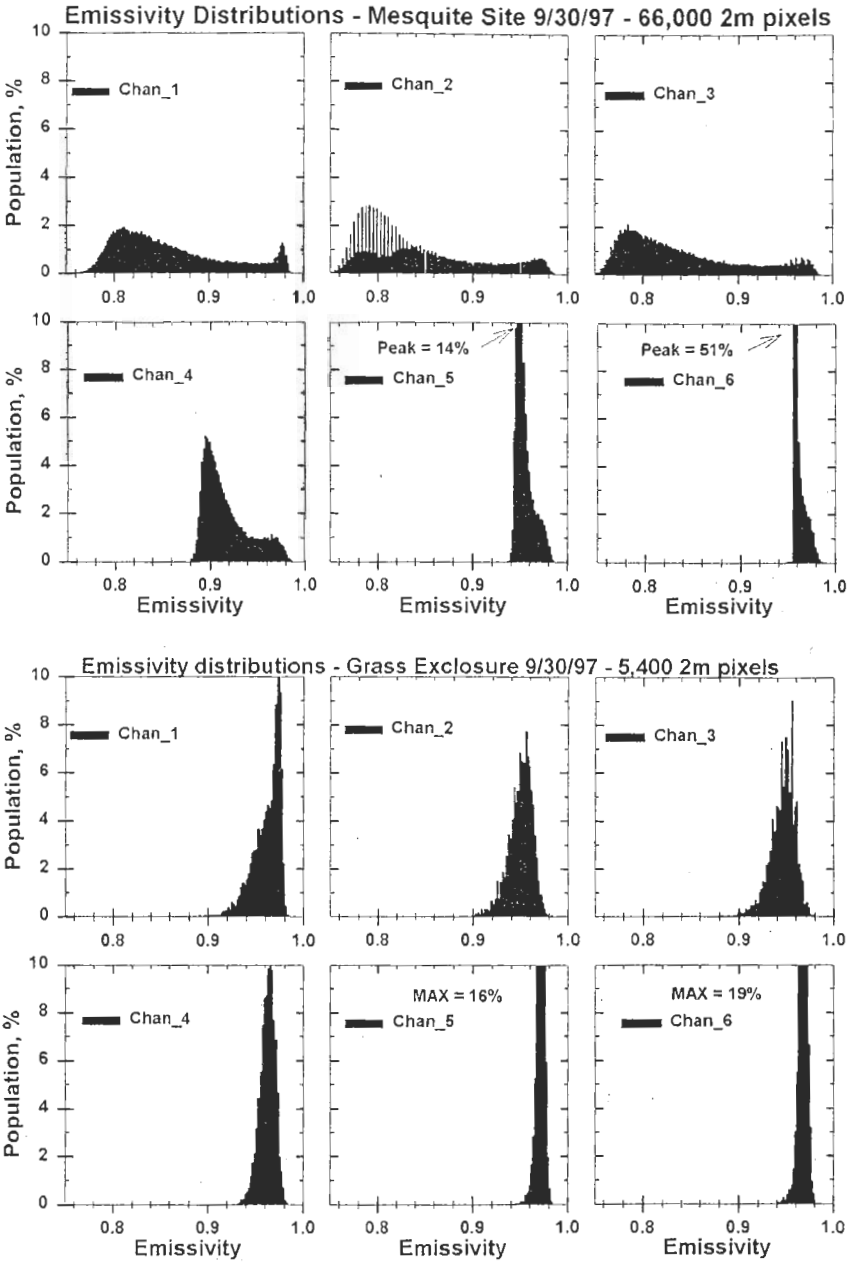

Fig. 3 Histograms of the emissivity distributions for the six TIMS channels for both the mesquite (top) and grass (bottom) sites.

The derived temperatures were compared with ground measurements from grids at both sites. The results show reasonable agreement, within 3°C for the mesquite site, when one considers that for bare soil the TIMS data sampled both the light and dark sands shown in Fig. 1. For the mesquite bush, the ground measurements were taken

looking into the side of bush which presumably will yield cooler temperatures (~3°C) than the straight-down view from the aircraft. At the grass grid the average of 49 measurements was within 1°C of the average of 400 pixels of aircraft data taken over the grid.

Acknowledgements This research was supported by the ASTER project of NASA's EOS-Terra program. The laboratory emissivity measurements were made by Cindy Grove of the Jet Propulsion Laboratory.

REFERENCES

Gillespie, A., Rokugawa, S., Matsunaga, T., Cothern, J. S., Hook, S. & Kahle, A. B. (1998) A temperature and emissivity separation algorithm for Advanced Spaceborne Thermal Emission and Reflection Radiometer (ASTER) images. *IEEE Trans. Geosci. & Remote Sens.* **36**, 1113–1126.

Salisbury, J. W. & D'Aria, D. M. (1992) Emissivity of terrestrial materials in the 8–14 mm atmospheric window. *Remote Sens. Environ.* **42**, 83–106.

Yamaguchi, Y., Kahle, A. B., Tsu, H., Kawakami, T. & Pniel, M. (1998) Overview of Advanced Spaceborne Thermal Emission and Reflection Radiometer (ASTER). *IEEE Trans. Geosci. & Remote Sens.* **36**, 1062–1071.